Eur. Phys. J. D **50**, 97–102 (2008)
DOI: 10.1140/epjd/e2008-00186-y

THE EUROPEAN PHYSICAL JOURNAL D

Electrons in a cryogenic planar Penning trap and experimental challenges for quantum processing

P. Bushev[1,2,a], S. Stahl[2], R. Natali[4], G. Marx[3], E. Stachowska[5], G. Werth[2], M. Hellwig[1], and F. Schmidt-Kaler[1]

[1] Quanten-Informationsverarbeitung, Universität Ulm, 89069 Ulm, Germany
[2] Institut für Physik, Johannes-Gutenberg-Universität Mainz, 55099 Mainz, Germany
[3] Ernst-Moritz-Arndt Universität Greifswald, Institut für Physik, 17489 Greifswald, Germany
[4] Dipartimento di Fisica, Università di Camerino, 62032 Camerino, Italy
[5] Poznan University of Technology, 60-965 Poznan, Poland

Received 30 June 2008 / Published online 3rd October 2008

Abstract. We report on trapping of clouds of electrons in a cryogenic planar Penning trap at $T \leq 100$ mK. We describe the experimental conditions to load, cool and detect electrons. Perspectives for the trapping of a single electron and for quantum information processing are given.

PACS. 37.10.-x Atom, molecule, and ion cooling methods – 03.67.Lx Quantum computation architectures and implementations

1 Introduction

In recent years, we have seen important progress in developing a quantum processor. Among the most advanced technologies are single ions in linear Paul traps. However, the hard problem of scalability of these devices remains, as we typically need to scale the system down to micrometer and even sub-micrometer size to construct a multi-qubit device. Strongly connected is the question of coherence: the lifetime of a superposition state needs to preserve a fixed phase relation over timescales much longer than the gate operation time. However, with the reduction in size of a quantum processor, the carriers of qubits come closer to the control electrodes so that any fluctuating electric fields are strongly limiting any processor already in the 100 μm range. It has been observed that decoherence effects are drastically reduced when operating the device at low temperatures [1,2]. These findings have triggered ideas for systems having the potential to avoid these problems.

We aim at employing single electrons confined in static Penning traps for quantum computation [3,4]. Electrons offer a two-level qubit system by the two spin orientations in a magnetic field. The cyclotron motion in a magnetic field of a few tesla can be cooled via synchrotron radiation and it has been experimentally demonstrated [5] that the cyclotron degree of freedom can be brought into the quantum mechanical ground state when the environmental temperature is kept below 100 mK. Electrons remain in this state for practically unlimited time. For a transfer of information between different qubits, realized by two single electrons stored in two different traps, an electric transmission line may transfer the voltage fluctuation induced in the trap electrodes by the electron oscillations. In the present paper we describe an experiment with a planar Penning trap geometry [6]. Arrays of planar traps for single electrons might satisfy two demands in developing a quantum processor: scalability and long coherence times [7]. The purpose of this article is to demonstrate the first experimental results with a planar Penning trap working inside a dilution refrigerator and to address future experimental challenges. After introducing the experimental setup, we describe the observation of a cold cloud of electrons. Pointing out the limitations of the present setup, we give an outlook to the trapping of a single electron and coupling of two qubits.

2 Experiment with planar traps

2.1 The Penning trap

A classical three dimensional Penning trap [8] consists of a quadrupole electrical potential Φ^{el} provided by a voltage U applied between a ring electrode and two electrically isolated end cap electrodes of hyperbolic shape, and a superimposed constant magnetic field B_0 along the z-axis.

$$\Phi^{el}(\rho, z) = \frac{U}{2r_0^2}(\rho^2 - 2z^2). \quad (1)$$

The characteristic dimension of the trap electrodes is denoted by r_0. For a properly chosen polarity the electric

[a] e-mail: pavel.bushev@uni-ulm.de

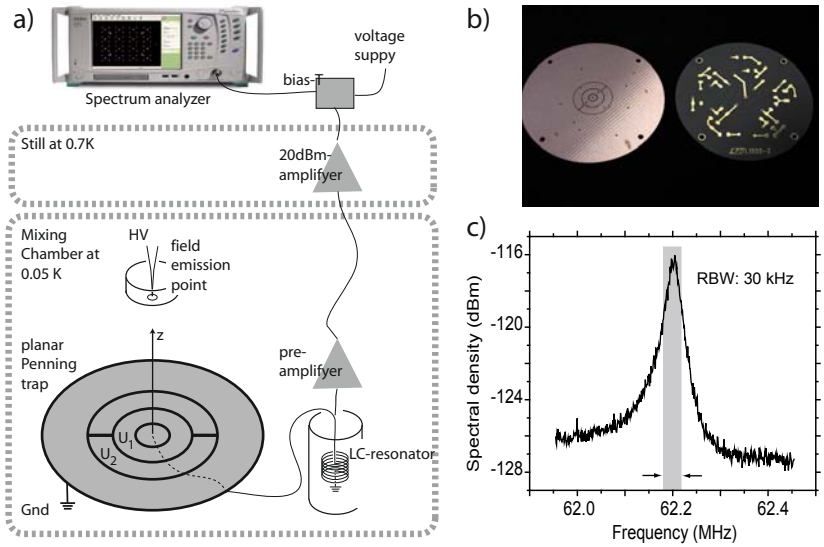

Fig. 1. (a) Sketch of the experimental setup: the planar trap consists of a central circular electrode on ground potential surrounded by two rings at voltages U_1 and U_2. The signal from the central electrode is resonantly enhanced, amplified in two stages and recorded on a spectrum analyzer. (b) Photo of the front and back side of the planar Penning trap used in the experiment. (c) Noise spectrum of the LC-circuit taken at $T \simeq 100$ mK. A resolution bandwidth of 30 kHz is indicated by a grey bar, this setting was used for the experiments described below.

field serves as confinement between the two end cap electrodes in the axial-direction (the z-axis) while the magnetic field prevents electron escape in the radial direction ρ. The equation of motion in this potential can be solved analytically and split into three harmonic oscillations at the frequencies

$$\omega_+ \approx \omega_c - \omega_z^2/2\omega_c \quad (2)$$

$$\omega_- \approx \omega_z^2/2\omega_c \quad (3)$$

$$\omega_z = \sqrt{2eU/md^2} \quad (4)$$

where $\omega_c = eB_0/mc$ is the free electrons cyclotron frequency, ω_+ is called the reduced cyclotron frequency, ω_- the magnetron frequency and ω_z the axial frequency. Characteristic values for these frequencies in our trap with planar geometry [6] are $\omega_+/(2\pi) \sim 60$ GHz, $\omega_-/(2\pi) \sim 30$ kHz and $\omega_z/(2\pi) \sim 60$ MHz when we apply a voltage $U \sim 7$ V and a magnetic field B_0 of 2.2 T.

The trap is placed inside the inner vacuum chamber (IVC) of a dilution refrigerator, no additional vacuum chamber is installed. A sketch of the setup is shown in Fig. 1a). The Penning trap itself consists of three concentric disk-electrodes, which are fabricated on standard FR-4 (epoxy) substrate, a 35 μm thick copper layer covered with a thin (0.5 μm) layer of gold. The electrodes are surrounded by a grounded plane. The innermost electrode is DC-grounded and is used for pick-up of the image charges induced by an electrons axial motion, while the other two electrodes serves to create the trapping potential. Voltages U_1 and U_2 are generated by 25 bit resolution low noise voltage source and applied to these electrodes. The diameter of the central electrode and the width of the trapping electrodes are equal to 2 mm. The total diameter of the trap including the surrounding grounded plane is 36 mm. The width of the gap between adjacent electrodes is about 100 μm. Low-pass filters and bias tees are placed on the back side of the trap and serve to feed in RF-excitation and DC signals. Metallized holes (vias) are used in this design to connect the top and bottom surfaces of the trap chip.

The outermost ring electrode (see Fig. 1) is split to allow magnetron excitation. The trap is installed on the bottom of the LC-resonator can, which is thermally connected to the mixing chamber. The inductance of the resonator is formed by a copper coil wound around a teflon cylinder mounted inside the copper can. The capacitance of the resonator is given by the stray capacitance (few picofarads) of the total setup and the input capacitor divider of the preamplifier. The quality factor of the LC-resonator at an operating temperature of 100 mK is about 1200, the resonance frequency is tuned to $\omega_{LC} = 2\pi \times 62.2$ MHz. The values of L and C are chosen such that the resonance frequency of the tank-circuit is close to the calculated value of ω_z. This tank circuit serves for a non-destructive electron detection.

The induced signal from the axial motion of trapped electrons is picked up by the resonator and processed by a low-noise HEMT-preamplifier [9], which is installed on the mixing chamber, then amplified by an additional 20 dB cryogenic amplifier mounted on the still plate at 0.7 K. The signal is then detected by a spectrum analyzer. The observed thermal noise of the LC-resonator is about 10 dB above the background noise. Under standard operating conditions at 100 mK, the power dissipation of the first amplification stage is about 90 μW. The cooling power of our dilution refrigerator is 130 μW seemed to be sufficient to work out the heat generated by the preamplifier. The noise temperature of the amplifier has been measured to

be about 5 K. It is also possible to work at even lower temperatures down to 50 mK by reducing the drain-current of the preamplifier, at the price by decreasing the observed signal-to-noise-ratio by about 4 dB.

For an excitation of the axial and magnetron degrees of freedom we apply signals from the top of the cryostat to the trap. The axial excitation is applied to the second ring, the magnetron excitation is applied to one of the halves of the outermost electrode.

A tungsten field emission point is installed above the trap and serves as a source of electrons. A small aperture is used to create an extraction field and as a guide for the emitted electrons. We capture secondary electrons, which are created by collisions of primary electrons with the residual gas.

2.2 Loading and detecting of an electron cloud

The planar trap is operated with both voltages U_1 and U_2 are set to +7 V and we calculate an axial potential with a depth of 4.5 eV. The super-conducting magnet is set to persistent mode at a magnetic field of 2.2 T and the amplifiers to standard operating conditions. The amplitude of the tank-circuit signal is measured with a spectrum analyzer at zero-span mode at a resonance frequency of 62.2 MHz with a resolution bandwidth (RBW) of 30 kHz, later referred to as the axial signal, Figure 1c.

To load electrons into the trap we apply for 1 to 2 s a DC-pulse of 800 V to the field emission point, which causes the spectrum analyzer signal to increase by a few dB, see Figure 2. After switching the field emission point off, the signal does not disappear but starts to increase on a time scale of seconds, giving evidence that electrons are trapped.

Initially trapped electrons are at high temperatures. The anharmonicity of the trapping potential results in an oscillation frequency below the detection frequency of the resonance circuit. The number of electrons at the beginning is large, therefore some of them oscillate in resonance with the detection circuit. A few seconds later, the electron cloud looses energy via its interaction with the tank-circuit and cools down. The electrons oscillation frequency increases and approaches the LC-resonance, here the axial signal reaches its maximum. Then the signal rapidly falls down to almost zero. The cloud of electrons cools down even further, the energy spread becomes smaller, the induced axial signal shifts out of resonance and we observe a rapid fall-off.

In Figure 2, two spectral density curves are taken with a RBW of 30 kHz, corresponding to different values of voltage applied on the second ring, while the voltage on the third ring remains unchanged $U_2 = 14$ V. Curve (a) is measured at $U_1 = 5.2$ V, which results according to our calculations in a trap frequency of $\omega_z/(2\pi) = 67.97$ MHz. For higher voltages, the trap is slightly steeper, and the calculated trap frequency is $\omega_z/(2\pi) = 66.38$ MHz. Therefore the signal reaches its maximum later in time, when the electron cloud energy has been cooled down so far that its axial oscillation reaches the detection resonance

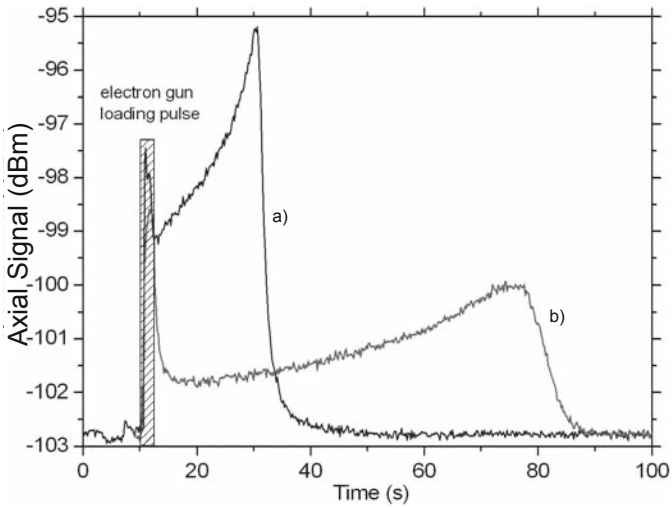

Fig. 2. Loading and trapping of clouds of electrons at different values of potential U_1. The data (a) were recorded at $U_1 = 5.2$ V, (b) at $U_1 = 4.8$ V. The RBW was set to 30 kHz.

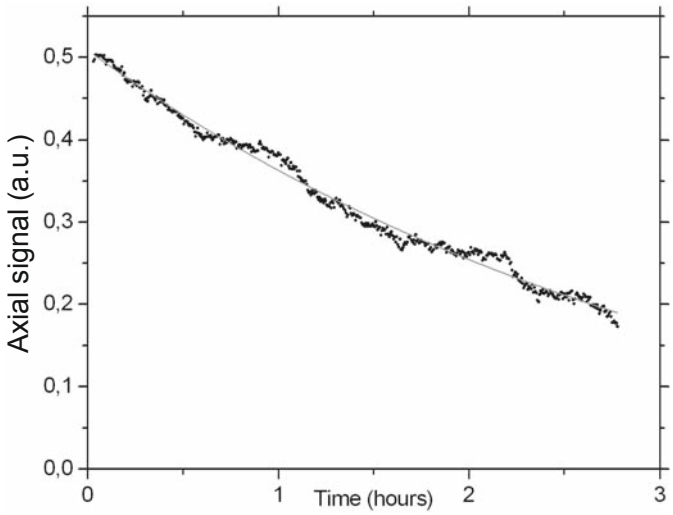

Fig. 3. Evolution of the axial signal during a resonant drive. The signal decays exponentially with a time constant of 3.5 h.

frequency. Once the axial signal is gone for a time of about 100 s after loading, we can re-excite their motion by applying a weak −80 dBm off-resonant (+60 kHz detuning) axial drive field to the second ring. The cloud heats up, a part of the cloud tunes to the tank resonance resonance frequency giving once more an enhanced axial signal. After turning the excitation off, the electrons cool down again with a time scale of seconds. We find that the number of electrons boiling-off from the trap decays with a time constant of a few hour. This value can be used to estimate an upper limit of the background IVC pressure at the position of the trap of 10^{-11} mbar. It was also possible to observe the axial signal for a long time while applying constantly a weak −80 dBm off-resonant (+80 kHz detuning) drive. Data are shown in Figure 3. The axial signal decays exponentially with a time constant of 3.5 h, confirming

the upper limit of the background pressure. For a more precise measurement of the pressure one has to perform a life-time measurement with a single or a few electrons.

2.3 Anharmonicity of the axial potential

A particular feature of the planar trap used in the present experiment is the lack of mirror symmetry around the potential minimum. This makes it impossible to create a genuinely harmonic potential. As a consequence the electron kinetic energy distribution is inhomogenously broadened and a spectrum analysis within a narrow RBW of a few Hz, as necessary for single electron detection, becomes impossible. For our trap we expect to detect a signal for a *single electron* with a RBW of a few Hz, but the broadening to 1 MHz reduces this signal by a factor of 10^5.

To quantify inhomogeneous broadening effects the frequency distribution of electrons inside the trap is measured. We slowly sweep the electrode voltage U_2 and record the axial signal. The data are presented in Figure 4. If the trap were perfectly harmonic, one would expect to observe a sharp peak which corresponds to a single axial oscillation frequency. In our case this peak is smeared out giving rise to a quite broad distribution, which can not only be associated with the large number of particles. This distribution corresponds to a broadening of ~ 3 MHz. It appeared impossible to adjust the voltages U_1 and U_2 to record a narrow resonance line.

To theoretically model such a frequency broadening, the trapping potential can be approximated by an anharmonic potential [10]

$$V(z) = \frac{1}{2}m\omega_z^2 z^2 + \varepsilon_3\left(\frac{z}{l}\right)^3 + \varepsilon_4\left(\frac{z}{l}\right)^4, \qquad (5)$$

where ε_3, and ε_4 are anharmonicity parameters and taken from an electrostatic CAD model of the trap, $l = \sqrt{\hbar/m\omega_z}$ is the spread of the electronic wave function in the ground state and ω_z is the frequency of an unperturbed oscillator. The energy levels of such an oscillator are calculated using perturbation theory. The correction to the energy distance between adjacent levels ΔE_n depends quadratically on quantum number n of the oscillator [10]

$$\Delta E_n = -\frac{15}{4}\frac{\varepsilon_3^2}{\hbar\omega_z}n^2 + \frac{3}{2}\varepsilon_4 n^2. \qquad (6)$$

The frequency broadening due to the anharmonicity of the potential $\Delta\gamma_{AH}$ can be calculated as

$$\Delta\gamma_{AH} \sim \frac{\partial\omega_z(E_n)}{\partial E_n}\langle E_z\rangle, \qquad (7)$$

where $\langle E_z\rangle = k_B T_z$ is the mean electron energy. Finally, for the frequency broadening we get

$$\Delta\gamma_{AH} = \frac{k_B T_z}{\hbar}\left\{-\frac{15}{2}\left(\frac{\varepsilon_3}{\hbar\omega_z}\right)^2 + 3\frac{\varepsilon_4}{\hbar\omega_z}\right\}. \qquad (8)$$

For the trap geometry and parameters used in our experiment a frequency broadening of γ_{AH} of about 3 MHz is expected and is in agreement with the measured data, see Figure 4. For optimized control voltages of $U_1 = -1$ V and $U_2 = 2.611$ V the anharmonicity is decreased to about 10 kHz, at the cost of a reduced trap depth by a factor of 50. This value is still about 3 orders of magnitude too large to allow observation of a single electron in our experiment. Even with this reduction of the frequency broadening one can not observe a single electron.

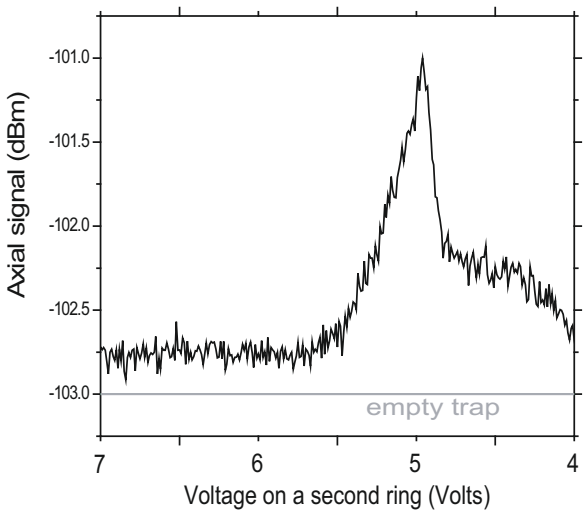

Fig. 4. Observation of an axial signal during a scan of the voltage on the second ring (U_2). Electron energy distributed over a large energy band. The solid gray line corresponds to the signal when no electrons are present in the trap.

In numerical and analytic simulations for more complex trap geometries including many rings addressed with different voltages U_i $(i = 1 \ldots 6)$, we found that equation (6) predicts a value not better than $\gamma_{AH} = 5$ kHz under typical operation conditions with $\omega_z \sim 100$ MHz and $T_z \sim 5$ K.

2.4 Parametric excitation of the electron cloud

Such a strong anharmonicity of the trapping potential allows us to observe the parametric resonance [11] of the trapped electron cloud. The first step is to load a cloud of electrons. A quite strong (−30 dB) excitation is applied to the second ring along the z-axis at a frequency $\omega_{exc} \sim 2\omega_{LC}$, in the experiment we use $\omega_{exc} = 124.35$ MHz. A clear sharp feature appears at the left side of the LC-resonance at $\omega_{exc}/2$, see Figure 5. The excitation frequency is chosen such that the parametric resonance appears a few tens of kHz detuned from the LC-circuit resonance frequency.

The observed parametric excitation arises from a nonlinear response of the electron cloud as the mixing product of the frequency of the electrons axial motion with ω_{exc}. The amplitude and the width of the observed parametric resonance is thus depending on the number of loaded

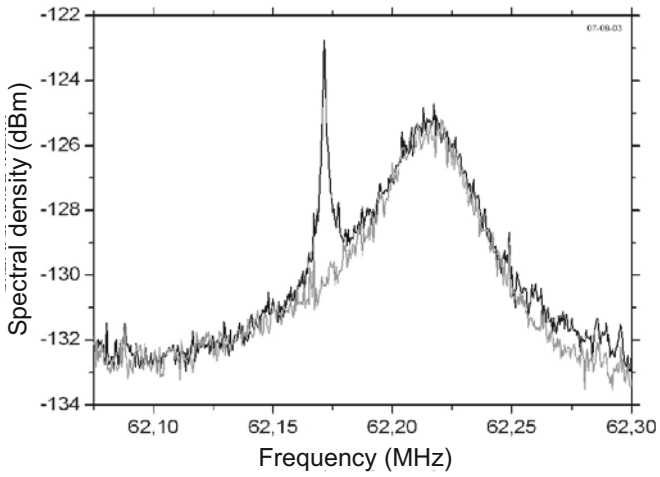

Fig. 5. Spectral noise of a tuned LC-circuit. The black line shows the response of electrons cloud to the parametric drive applied to one of the electrodes of the planar trap. For comparison a scan without trapped electrons, showing the empty resonance of the tank-circuit (grey line).

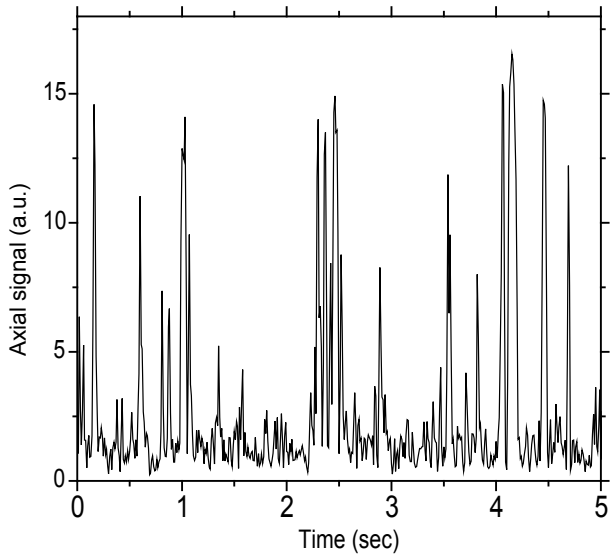

Fig. 6. Time evolution of the amplitude of the parametric resonance. Clearly separated bursts are likely being associated with the excitation of only a few electrons. RBW = 30 Hz.

electrons. When we reduce the number of particles, we observe a parametric resonance as narrow as 3 Hz. At such conditions, the excited parametric signal is not stable with time, but shows separated bursts, see Figure 6. Each burst usually lasts a few milliseconds and then disappears and appears again. Such peaks can be associated with few electrons excitation or even perhaps with excitation of a single electron. Nevertheless, it cannot be stated as proof of a single electron excitation and detection.

3 Conclusion and outlook

To detect a single electron in a planar trap, the frequency broadening $\Delta\gamma_{AH}$ has to be at most one Hertz. Under that condition, a single electron "dip" has been observed associated with its axial motion [13], or narrow resonance peak has been obtained using two-frequency detection method [14,15]. One way to fulfill this condition is to reduce the axial temperature T_z, see equation (7). If lowered by three orders of magnitude, from 5 K down to values of what can be reached with powerful dilution fridges (5 mK), one expects $\Delta\gamma_{AH} \sim 10$ Hz. Here, the main challenge is that the present detection technique is based on the electrical coupling between a single electron and the effective resistance the LC tank circuit. The oscillating electron acquires the temperature of this resistor, which was observed to be a few kelvins [13]. The temperature of resistor is larger than the temperature of cryostat environment due to electrical connection of LC tank circuit to the input of the preamplifier (see Fig. 1a), thereby acquiring an influence of the transistor thermal noise, which becomes a serious problem for most experiments. Therefore this resistance stays at the temperature of the pre-amplifier, which can hardly be lowered below 1 K [9,13,16,17]. For example, in an experiment with a single electron conducted in Harvard [13,18], the axial temperature was about 4 K, despite all efforts. For precise measurements, a "dark detection"-method is used, where amplifiers are turned off during the manipulation of the spin and cyclotron states, thus reducing the axial temperature of the electron by more than order of magnitude [18].

Another way to detect a single particle is to use a trap with improved field geometry [12]. With a proper choice of the trap geometry and applied voltages, the anharmonicity parameters in equation (6) can be eliminated giving no frequency broadening. Nevertheless, the reduction of the trap size to a fraction of a millimeter makes coupling to the external tank-circuit stronger ($\sim 1/r_0^2$) allowing us to observe a single particle in a trap, even when its geometry is not optimized. Under these conditions the coupling of two individually trapped electrons by wire appears to be feasible for quantum information processing [7,19,20].

To summarize, we have demonstrated the first planar cryogenic Penning trap working below 100 mK. With the present trap we have succeeded in cooling and detecting a cloud of electrons. The experiment requires no additional vacuum chamber inside the IVC, contrary to most Penning trap experiments. Our measured trap lifetime is 3.5 h, making further development of the experiment towards quantum computing possible. The strong anharmonicity of the axial potential in the planar trap prevented us from observing a single electron but allowed to reveal nonlinear phenomena like parametric resonance.

P. Bushev thanks Maxim Efremov for very stimulating discussions. We acknowledge financial support by the European commission (project QUELE grant number FP6-003772) and the German Science Foundation within the project SFB-TRR21.

References

1. L. Deslauriers et al., Phys. Rev. Lett. **97**, 103007 (2006)
2. J. Labaziewicz et al., Phys. Rev. Lett. **100**, 013001 (2008)
3. G. Ciaramicoli et al., Phys. Rev. A **63**, 052307 (2001)
4. S. Manchini et al., Phys. Rev. A **61**, 012303 (2000)
5. S. Peil, G. Gabrielse, Phys. Rev. Lett. **83**, 1287 (1999)
6. S. Stahl et al., Eur. Phys. J. D **32**, 139 (2005)
7. G. Ciaramicoli et al., Phys. Rev. Lett. **91**, 017901 (2003)
8. L.S. Brown, G. Gabrielse, Rev. Mod. Phys. **58**, 233 (1986)
9. R.F. Bradley, Nucl. Phys. B (Proc. Suppl.) **72**, 137 (1999) and references therein
10. S. Flügge, *Practical Quantum Mechanics* (Springer, Berlin-Heidelberg, 1999)
11. L.D. Landau, E.M. Lifshitz, *Course of Theoretical Physics, Vol. 1: Mechanics* (Butterworth-Heinemann, 1976)
12. G. Gabrielse, F.C. MacKintosh, Int. J. Mass Spectrom. Ion Proc. **57**, 1 (1984)
13. B. D'Urso et al., Phys. Rev. Lett. **90**, 043001 (2003)
14. D. Wineland et al., Phys. Rev. Lett. **31**, 1279 (1973)
15. J. Tan, G. Gabrielse, Appl. Phys. Lett. **55**, 2144 (1989)
16. N. Oukhanski et al., Rev. Sci. Instrum. **74**, 1145 (2003)
17. L. Roschier, P. Hakonen, Cryogenics **44**, 783 (2004)
18. B. Odom et al., Phys. Rev. Lett. **97**, 030801 (2006)
19. A. Sørensen et al., Phys. Rev. Lett. **92**, 063601 (2004)
20. J. Zurita-Sánchez, C. Henkel, to be published